Closed-form Polarimetric Two-Scale Model for sea scattering evaluation

Gerardo Di Martino, Alessio Di Simone, Antonio Iodice, Daniele Riccio
Department of Information Technology and Electrical Engineering,
University of Naples, "Federico II", Naples, Italy.

***Abstract*—Among the methods to compute scattering from rough surfaces, the Two-Scale Model (TSM) is a good compromise between range of validity and accuracy on one hand, and efficiency on the other hand. In fact, its range of validity is the union of those of the Geometrical Optics (GO) and of the small perturbation method (SPM). On the other hand, if one is interested only in copolarized normalized radar cross section, a combination of the analytical closed form expressions of GO and SPM can be used, so that high efficiency is obtained. However, if a fully polarimetric analysis of the scattering must be performed, a numerical integration is needed, which strongly reduces the efficiency. Recently, some of the authors of this work developed an approximated closed-form expression of such an integral, and then of the fully polarimetric version of TSM, that was named Polarimetric TSM (PTSM). However, this expression was only obtained for statistically isotropic rough surfaces and in the backscattering configuration. In this work we present the rationale for the extension to anisotropic roughness and to the bistatic configuration, aimed at evaluating scattering from the sea surface. Results are shown for anisotropic surfaces in the backscattering case and for isotropic surfaces in the bistatic scattering case. They can be usefully employed in sea state monitoring via microwave remote sensing systems.**

Keywords—electromagnetic scattering from rough surfaces; sea surface scattering

I. INTRODUCTION

Methods for the evaluation of scattering from rough surfaces can be classified as numerical, such as the Method of Moments (MoM) [1], approximate analytical/numerical, such as the Small Slope Approximation (SSA) [2] and its second-order version (SSA2) [3], or the Two-Scale Model (TSM) [4-5], and approximate closed-form, such as the Small Perturbation Method (SPM) [6], the Geometrical Optics (GO) [6] or empirical methods [7]. The three categories are listed in order of increasing efficiency and decreasing validity range and accuracy. A good compromise between range of validity and accuracy on one hand, and efficiency on the other hand, is provided by TSM. According to this model, the scattering rough surface is represented as the superposition of a small-scale roughness, at horizontal scale of the order of wavelength, and a large-scale roughness, at horizontal scale large with respect to wavelength. Scattering from small-scale roughness is computed by using the SPM, and it mainly depends on small-scale roughness spectrum, whereas scattering from large-scale roughness is evaluated by using GO, and it mainly depends on large-scale roughness root mean square (rms) slopes. The former is dominant in far-from-specular directions, whereas the latter is dominant in near-specular directions. Accordingly, the range of validity of TSM is the union of the GO and SPM ones. On the other hand, if one is interested only in copolarized normalized radar cross section (NRCS), a combination of the analytical closed form expressions of GO and SPM can be used, so that a high computation efficiency is obtained. However, if a fully polarimetric analysis of the scattering must be performed, so that cross-polarization and de-polarization effects must be modelled, then the SPM expression of scattering from small-scale roughness must be averaged over the surface slopes of the large-scale roughness. This average operation requires a numerical integration that strongly reduces the computation efficiency. Recently, some of the authors of this work developed an approximated closed-form expression of such an integral, and then of the fully polarimetric version of TSM, that was named Polarimetric TSM (PTSM) [8-10]. However, that expression was only obtained for statistically isotropic rough surfaces and in the backscattering (i.e., monostatic) configuration. In this work we present the generalization of the isotropic monostatic PTSM of [8-10] in two directions: towards an anisotropic monostatic PTSM and towards an isotropic bistatic PTSM. Both generalizations are applied to the evaluation of scattering from the sea surface.

This paper is organized as follows. Section II presents the employed description of the sea surface. The anisotropic monostatic PTSM presented in section III, while the isotropic bistatic PTSM is introduced in Section IV. Finally, Conclusions are drawn in section V.

II. SEA SURFACE MODEL

In order to implement the TSM, the small-scale surface roughness must be described by specifying its power spectral density (PSD), briefly referred to as surface spectrum. Different sea surface spectra have been proposed in literature; however, recently for electromagnetic scattering computations the Elfouhaily spectrum [11] is very often employed. Therefore, for the small-scale roughness we here use the high-frequency part of the Elfouhaily spectrum:

978-1-7281-3815-2/19/$31.00 ©2019 IEEE

$$W_{2D}(\kappa,\varphi) = W(\kappa)\Phi(\kappa,\varphi) \tag{1}$$

where κ is the amplitude of the surface wavenumber vector and φ is the angle between the surface wavenumber vector and the x axis (see Fig. 1),

$$W(\kappa) = \frac{\pi \alpha_m c_m}{c\,\kappa^4} \exp\left[-\frac{1}{4}\left(\frac{\kappa}{\kappa_m}-1\right)^2\right] \tag{2}$$

where

$$\alpha_m = \begin{cases} 0.01\left[1+\ln\left(u^*/c_m\right)\right] & \text{for } u^* \le c_m \\ 0.01\left[1+3\ln\left(u^*/c_m\right)\right] & \text{for } u^* > c_m \end{cases}, \tag{3}$$

$\kappa_m = 363 \text{ m}^{-1}$, $c_m = 0.23$ m/s , c is the sea-wave phase velocity

$$c = \sqrt{\frac{g}{\kappa}\left[1+\left(\frac{\kappa}{\kappa_m}\right)^2\right]}, \tag{4}$$

g = 9.81 m/s^2 being the gravity acceleration, and u^* is the friction velocity

$$u^* = \sqrt{C_d}\; u_{10} \quad , \tag{5}$$

with u_{10} being the wind velocity at 10 m height and

$$C_d = \begin{cases} 1.205\cdot 10^{-3} & \text{for } 4 \le u_{10} < 11 \text{ m/s} \\ \left(0.49+0.065u_{10}\right)10^{-3} & \text{for } 11 \le u_{10} \le 25 \text{ m/s} \end{cases}; \tag{6}$$

finally,

$$\Phi(\kappa,\varphi) = 1+\Delta(\kappa)\cos\left[2\left(\varphi_w-\varphi\right)\right] \quad , \tag{6}$$

where

$$\Delta(\kappa) = \tanh\left[0.173+4\left(c/c_p\right)^{2.5}+a_m\left(c_m/c\right)^{2.5}\right] \quad , \tag{7}$$

with $c_p \cong u_{10}/0.84$ and $a_m = 0.13u^*/c_m$, and φ_w is the angle between wind direction and the x axis. It is worth noticing that, assuming $c \cong \sqrt{g/\kappa}$, eq. (2) is well approximated by the isotropic power-law PSD employed in [8-10], with Hurst coefficient H_f=0.75 .

With regard to the large-scale roughness, the implementation of the TSM requires that it is described via the probability density function (pdf) of its slopes along x and y directions.

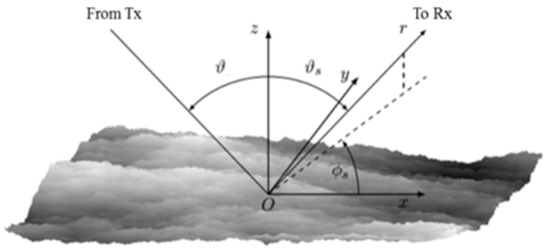

Figure 1: Geometry of the problem and coordinate system

Sea surface slopes along up-wind and cross-wind directions, s_{up} and s_{cross}, are, with good approximation, zero-mean independent Gaussian random variables with variances σ_{up}^2 and σ_{cross}^2, respectively [12]. The latter depend both on physical factors like wind speed, and on the incident electromagnetic frequency, and hence wavelength, that defines the cut-off scale between small- and large-scale roughness. However, these slope variances can be computed by using the semiempirical evaluation of [13], that holds at a frequency of 1.5 GHz:

$$\begin{aligned} \sigma_{up}^2 &= 0.45\left[0.00316 f\left(u_{10}\right)\right] \\ \sigma_{cross}^2 &= 0.45\left[0.003+0.00192 f\left(u_{10}\right)\right] \end{aligned} \tag{8}$$

where

$$\begin{aligned} f\left(u_{10}\right) &= u_{10} && \text{for } 0 < u_{10} \le 3.49 \\ f\left(u_{10}\right) &= 6\ln\left(u_{10}\right) && \text{for } 3.49 < u_{10} \le 46 \\ f\left(u_{10}\right) &= 0.411u_{10} && \text{for } 46 < u_{10} \end{aligned} \quad . \tag{9}$$

Proper corrections to these values, to deal with different microwave frequencies, can be made along the lines described in [14].

Starting from (8-9), it turns out that surface slopes along x and y directions are zero-mean jointly Gaussian random variables with variances

$$\begin{aligned} \sigma_x^2 &= \frac{1}{2}\left[\sigma_{up}^2+\sigma_{cross}^2+\left(\sigma_{up}^2-\sigma_{cross}^2\right)\cos 2\varphi_w\right] \\ \sigma_y^2 &= \frac{1}{2}\left[\sigma_{up}^2+\sigma_{cross}^2-\left(\sigma_{up}^2-\sigma_{cross}^2\right)\cos 2\varphi_w\right] \end{aligned} \tag{10}$$

and correlation coefficient

$$\rho = \frac{1}{2}\sin 2\varphi_w \frac{\sigma_{cross}^2-\sigma_{up}^2}{\sigma_x\sigma_y} \quad . \tag{11}$$

III. ANISOTROPIC MONOSTATIC PTSM

By using the TSM approach, the overall scattering surface can be seen as a collection of randomly rough facets, whose roughness is the small-scale roughness, randomly tilted

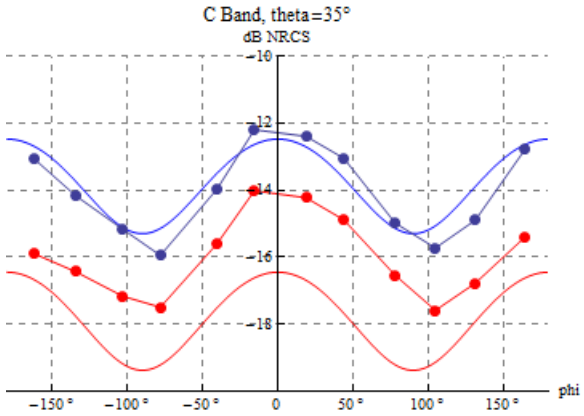

Figure 2: Copolarized NRCS dependence on wind direction φ_w at C band (frequency = 5.66 GHz, $\varepsilon = 67 - j36$), $\vartheta = 35°$, and $u_{10} = 10$ m/s. Computed *vv* (blue line) and *hh* (red line) NRCS and corresponding measured data (blue and red connected dots).

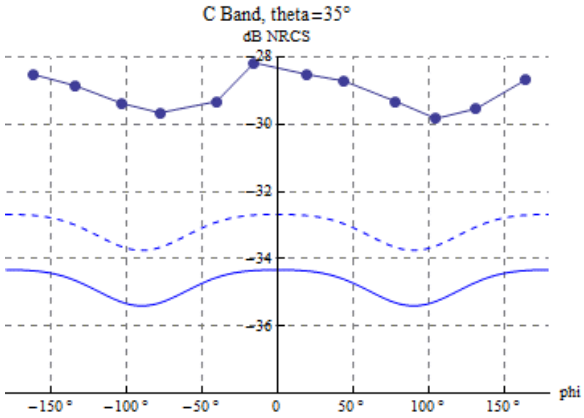

Figure 3: Crosspolarized NRCS dependence on wind direction φ_w at C band (frequency = 5.66 GHz, $\varepsilon = 67 - j36$), $\vartheta = 35°$, and $u_{10} = 10$ m/s. Computed *hv* NRCS obtained via proposed PTSM (solid line) and via SSA2-A [15] (dashed line), and corresponding measured data (connected dots).

according to the slope of the large-scale roughness. Scattering by the tilted rough facet is computed by using the SPM, and the NRCS of the overall surface is obtained by averaging the tilted facet NRCS with respect to facet random slopes. In [8-10] a closed form evaluation of this average was obtained in the backscattering case by performing a series expansion of NRCS around zero slopes. However, there a statistically isotropic surface was considered, i.e., it was assumed that $\Phi(\kappa,\varphi) = 1$ and that $\sigma_{up}^2 = \sigma_{cross}^2$, so that $\sigma_x^2 = \sigma_y^2 = \sigma^2$ and $\rho = 0$. Here we remove those assumptions. Key points of the presented approach are: 1) expressing the local incidence angle ϑ_{li}, and the rotation angle β_i of the incidence plane, in terms of the global incidence angle ϑ_i and of local surface slopes s_x and s_y; 2) expanding tilted facet SPM NRCS expressions in power series of facet slopes; and 3) averaging with respect to facet slopes. Details of the mathematical derivation are reported in [14]. We here report the final results, in terms of the elements

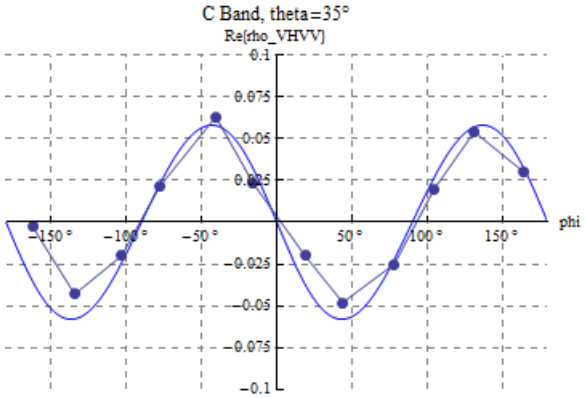

Figure 4: Crosspol-copol correlation dependence on wind direction φ_w at C band (frequency = 5.66 GHz, $\varepsilon = 67 - j36$), $\vartheta = 35°$, and $u_{10} = 10$ m/s. Real part of the *vh,vv* correlation coefficient (blue line) and corresponding measured data (blue connected dots).

of the polarimetric covariance matrix, $R_{pq,rs}$, where the subscripts p, q, r, s may each stand for h (horizontal polarization) or v (vertical polarization), so that $R_{pq,pq}$ is the NRCS σ_{pq}^0 at pq polarization. For the large-scale contribution, we employ the usual GO expression:

$$R_{pq,rs}^{large} = \begin{cases} \dfrac{|\Gamma|^2}{2\sigma_x\sigma_y\sqrt{1-\rho^2}\cos^4\vartheta}\exp\left\{-\dfrac{\tan^2\vartheta}{2(1-\rho^2)\sigma_x^2}\right\} & \text{if } p=q \text{ and } r=s \\ 0 \quad \text{otherwise} \end{cases} \tag{12}$$

Γ being the Fresnel coefficient at normal incidence, whereas for the small-scale one we get

$$\begin{cases} \sigma_{hh}^{0small} = \Theta_{hh}(\vartheta)\Phi(2k\sin\vartheta,0)\left[1+\dfrac{C_{0,2}^{hh}}{\Theta_{hh}(\vartheta)}\sigma_x^2+\left(\dfrac{C_{2,0}^{hh}}{\Theta_{hh}(\vartheta)}+2\dfrac{\mathrm{Re}\{F_v(\vartheta)/F_h(\vartheta)\}-1}{\sin^2\vartheta}\right)\sigma_y^2\right] \\ \sigma_{vv}^{0small} = \Theta_{vv}(\vartheta)\Phi(2k\sin\vartheta,0)\left[1+\dfrac{C_{0,2}^{vv}}{\Theta_{vv}(\vartheta)}\sigma_x^2+\left(\dfrac{C_{2,0}^{vv}}{\Theta_{vv}(\vartheta)}-2\dfrac{1-\mathrm{Re}\{F_h(\vartheta)/F_v(\vartheta)\}}{\sin^2\vartheta}\right)\sigma_y^2\right] \\ \sigma_{hv}^{0small} = \Theta_{hv}(\vartheta)\Phi(2k\sin\vartheta,0)\dfrac{|F_v(\vartheta)-F_h(\vartheta)|^2}{F_h(\vartheta)F_v^*(\vartheta)\sin^2\vartheta}\sigma_y^2 \\ R_{hh,vv}^{small} = \Theta_{hv}(\vartheta)\Phi(2k\sin\vartheta,0) \\ \qquad \left[1+\dfrac{C_{0,2}^{hv}}{\Theta_{hv}(\vartheta)}\sigma_x^2+\left(\dfrac{C_{2,0}^{hv}}{\Theta_{hv}(\vartheta)}+\dfrac{F_h^*(\vartheta)/F_v^*(\vartheta)+F_v(\vartheta)/F_h(\vartheta)-2}{\sin^2\vartheta}\right)\sigma_y^2\right] \\ R_{hh,hv}^{small} = \Theta_{hv}(\vartheta)\Phi(2k\sin\vartheta,0)\left[\dfrac{(1-F_h^*(\vartheta)/F_v^*(\vartheta))\cot\vartheta}{\sin\vartheta}+\dfrac{(C_{0,1}^{hv}-C_{0,1}^{hh})}{\Theta_{hv}(\vartheta)\sin\vartheta}\right]\rho\sigma_x\sigma_y \\ R_{hv,vv}^{small} = \Theta_{hv}(\vartheta)\Phi(2k\sin\vartheta,0)\left[\dfrac{(F_v(\vartheta)/F_h(\vartheta)-1)\cot\vartheta}{\sin\vartheta}+\dfrac{(C_{0,1}^{vv}-C_{0,1}^{hv})}{\Theta_{hv}(\vartheta)\sin\vartheta}\right]\rho\sigma_x\sigma_y \end{cases} \tag{13}$$

where

$$\Theta_{pq}(\vartheta) = \frac{4}{\pi}k^4\cos^4\vartheta W(2k\sin\vartheta)F_p(\vartheta)F_q^*(\vartheta) \tag{14}$$

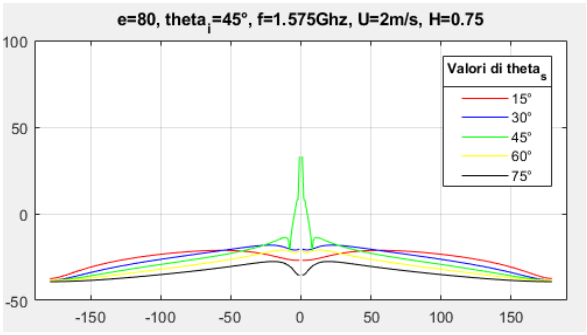

Figure 5: RR-polarized NRCS as a function of the scattering azimuthal angle φ_s at L band (frequency = 1.575 GHz, $\varepsilon = 80$), $\vartheta_i = 35°$, and $u_{10} = 2$ m/s.

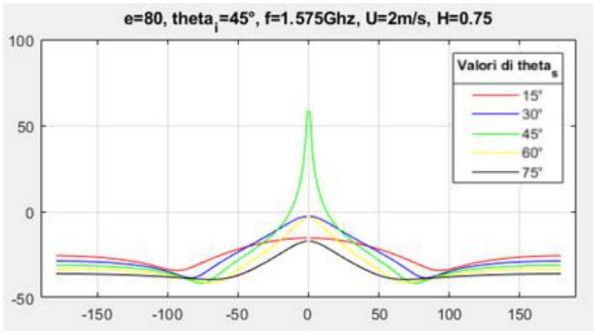

Figure 6: RL-polarized NRCS as a function of the scattering azimuthal angle φ_s at L band (frequency = 1.575 GHz, $\varepsilon = 80$), $\vartheta_i = 35°$, and $u_{10} = 2$ m/s.

$\vartheta = \vartheta_i = \vartheta_s$, F_h and F_v are the Bragg coefficients at horizontal and vertical polarization, and expansion coefficients $C_{k,n}^{pq}$ are reported in [8] and [14].

Some numerical results, with comparison with real data reported in [3] and with other methods results, are shown in Figs. 2-4. For further results, and for full discussion of the comparison, the reader is referred to [14].

IV. Isotropic Bistatic PTSM

The key point to generalize PTSM of [8-10] to the bistatic case is to express in terms of ϑ_i, s_x and s_y not only the local incidence angle ϑ_{li} and the incidence plane rotation angle β_i, but also scattering angles ϑ_{ls}, φ_{ls}, and the rotation angle β_s of the scattering plane. The expressions of ϑ_{ls}, φ_{ls}, and β_s as functions of ϑ_i, s_x and s_y are not available in literature, and are an original contribution of this work. They are reported in the following:

$$\cos\vartheta_{ls} = \frac{-s_y \sin\vartheta_s \sin\varphi_s - s_x \sin\vartheta_s \cos\varphi_s + \cos\vartheta_s}{\sqrt{1+s_x^2+s_x^2}} \qquad (15)$$

$$\cos\varphi_{ls} = \frac{\left(\hat{k}_i \times \hat{n}_l\right)}{\left|\hat{k}_i \times \hat{n}_l\right|} \cdot \frac{\left(\hat{k}_s \times \hat{n}_l\right)}{\left|\hat{k}_s \times \hat{n}_l\right|} = \frac{1}{\sqrt{(\sin\vartheta_i - s_x\cos\vartheta_i)^2 + {s_y}^2}}$$

$$\left(\frac{(\sin\vartheta_i - s_x\cos\vartheta_i)(\sin\vartheta_s\cos\varphi_s + s_x\cos\vartheta_s)}{\sqrt{(\sin\vartheta_s\cos\varphi_s + s_x\cos\vartheta_s)^2 + (-s_y\cos\vartheta_s - \sin\vartheta_s\sin\varphi_s)^2 + (-s_x\sin\vartheta_s\sin\varphi_s + s_y\sin\vartheta_s\cos\varphi_s)^2}} + \right.$$

$$\left. + \frac{s_y\cos\vartheta_i(-s_y\cos\vartheta_s - \sin\vartheta_s\sin\varphi_s) + s_y\sin\vartheta_i(-s_x\sin\vartheta_s\sin\varphi_s + s_y\sin\vartheta_s\cos\varphi_s)}{\sqrt{(\sin\vartheta_s\cos\varphi_s + s_x\cos\vartheta_s)^2 + (-s_y\cos\vartheta_s - \sin\vartheta_s\sin\varphi_s)^2 + (-s_x\sin\vartheta_s\sin\varphi_s + s_y\sin\vartheta_s\cos\varphi_s)^2}} \right) \qquad (16)$$

$$\tan\beta_s = \frac{s_y\cos\varphi_s - s_x\sin\varphi_s}{s_y\cos\vartheta_s\sin\varphi_s + s_x\cos\vartheta_s\cos\varphi_s + \sin\vartheta_s} \qquad (17)$$

Once these relations are obtained, a procedure similar to the one of the monostatic case can be followed: 1) express the local incidence ϑ_{li} and scattering ϑ_{ls}, φ_{ls} angles, and rotation angles β_i and β_s of incidence and scattering planes, in terms of global incidence ϑ_i and scattering ϑ_s, φ_s angles and of local surface slopes s_x and s_y; 2) expand tilted facet SPM NRCS expressions in power series of facet slopes; and 3) average with respect to facet slopes. The complete mathematical formulation will be provided at the conference. Here we report some numerical results. In particular, in Figs. 5-6 we consider the NRCS expressed in circular polarization basis (R and L stand for right-handed and left-handed circular polarizations, respectively), which is of interest in some polarimetric Synthetic Aperture Radar (SAR) configuration (e.g., compact pol) and for Global Navigation Satellite System Reflectometry (GNSS-R).

V. Conclusion

In this work, the isotropic monostatic PTSM introduced in [8-10] has been generalized to the anisotropic monostatic and isotropic bistatic cases and applied to scattering from the sea surface, modelled by using the directional Elfouhaily spectrum and an anisotropic jointly Gaussian distribution of surface slopes. Closed-form expressions of all the elements of the polarimetric covariance matrix, including NRCSs, have been obtained. Comparison with real data, performed in the anisotropic monostatic case, shows that the agreement of the proposed method with real data is similar to the one of other, more refine but less efficient, methods.

Obtained formulations can be useful in devising sea state retrieval methods that employ data from microwave remote sensing systems, such as polarimetric SAR and GNSS-R.

References

[1] J. T. Johnson, R. T. Shin, J. A. Kong, L. Tsang, and K. Pak, "A numerical study of the composite surface model for ocean backscattering," *IEEE Trans. Geosci. Remote Sensing*, vol. 36, pp. 72–83, Jan. 1998.

[2] A. Voronovich, "Small-slope approximation for electromagnetic wave scattering at a rough interface of two dielectric half-spaces", Waves in Random Media, vol. 4, pp. 337-367, 1994.

[3] A. G. Voronovich and V. U. Zavorotny, "Full-polarization modeling of monostatic and bistatic radar scattering from a rough sea surface", *IEEE Trans. Antennas Propag.*, vol. 62, no. 3, pp. 1362–1371, March 2014.

[4] J. W. Wright, “A New Model for Sea Clutter”, *IEEE Trans. Antennas Propag.*, vol. 16, pp. 217-223, 1968.

[5] G. R. Valenzuela, “Scattering of Electromagnetic Waves from a Tilted Slightly Rough Surface”, *Radio Sci.*, vol. 3, pp. 1057-1066, 1968.

[6] F. T. Ulaby, R. K. Moore, and A. K. Fung, *Microwave Remote Sensing*. Reading, MA: Addison-Wesley, 1982.

[7] Y. Oh, K. Sarabandi, and F. T. Ulaby, ‘‘An empirical model and an inversion technique for radar scattering from bare soil surfaces,’’ *IEEE Trans. Geosci. Remote Sens.*, vol. 30, no. 2, pp. 370–381, Mar. 1992.

[8] A. Iodice, A. Natale, and D. Riccio, “Retrieval of Soil Surface Parameters via a Polarimetric Two-Scale Model”, *IEEE Trans. Geosc. Remote Sens.*, vol. 49, no. 7, pp. 2531-2547, July 2011.

[9] A. Iodice, A. Natale, and D. Riccio, “Polarimetric two-scale model for soil moisture retrieval via dual-pol HH-VV SAR data,” *IEEE J. Sel. Topics Appl. Earth Observ.*, vol. 6, no. 3, pp. 1163–1171, Jun. 2013.

[10] G. Di Martino, A. Iodice, A. Natale, D. Riccio, "Polarimetric Two-Scale Two-Component Model for the Retrieval of Soil Moisture Under Moderate Vegetation via L-Band SAR Data", *IEEE Trans. Geosc. Remote Sens.*, vol.54, no.4, pp. 2470-2491, 2016.

[11] T. Elfouhaily, B. Chapron, K. Katsaros, and D. Vandemark, “A unified directional spectrum for long and short wind-driven waves,” *J. Geophys. Res.*, vol. 102, pp. 15781–15796, 1997.

[12] C. S. Cox and W. Munk, “Measurement of the roughness of the sea surface from photographs of the sun’s glitter”, *J. Opt. Soc. Am.*, vol. 44, pp. 838–850, 1954.

[13] S. J. Katzberg, O. Torres, G. Ganoe, “Calibration of reflected GPS for tropical storm wind speed retrievals”, *Geophys. Res. Lett.*, vol.33, L18602, pp. 1-5, 2006.

[14] G. Di Martino, A. Iodice, D. Riccio, “Closed-Form Anisotropic Polarimetric Two-Scale Model for Fast Evaluation of Sea Surface Backscattering”, *IEEE Trans. Geosc. Remote Sens.*, in print.

[15] C. A. Guérin and J. T. Johnson, “A simplified formulation for rough surface cross-polarized backscattering under the second-order small-slope approximation”, *IEEE Trans. Geosc. Remote Sens.*, vol. 53, no. 11, pp. 6308–6314, Nov. 2015.